PAPER

Check for updates

Clicking beyond suspensions: understanding thiol–ene chemistry on solid-supported MoS₂†

Miriam C. Rodríguez González, [a,b] Iván M. Ibarburu, [c] Clara Rebanal, [c] Manuel Vázquez Sulleiro, [d] Rahul Sasikumar, [a] Alicia Naranjo, [d] Cosme G. Ayani, [c] Manuela Garnica, [d] Fabián Calleja, [d] Emilio M. Pérez, *[d] Amadeo L. Vázquez de Parga *[c,d,e] and Steven De Feyter *[a]

Molecular functionalization of MoS₂ has attracted a lot of attention due to its potential to afford fine-tuned hybrid materials that benefit from the power of synthetic chemistry and molecular design. Here, we report on the on-surface reaction of maleimides on bulk and molecular beam epitaxy grown single-layer MoS₂, both in ambient conditions as well as ultrahigh vacuum using scanning probe microscopy.

Introduction

Molybdenum disulfide (MoS₂) has become an interesting 2D material due to its exceptional properties and their applications in electronic and optoelectronic,[1,2] biosensing,[3] catalysis[4] or energy storage[5] among others.[6–8] Surface functionalization of this material with organic moieties has been targeted to improve the processability of bulk dispersions and to tune the resulting changes of the physicochemical properties.[9] In this context, different approaches have been reported employing molecular species through non-covalent and covalent interactions, generally in dispersions. Among them, protocols leading to a covalent bond between the modifier and the surface have gained attention due to the robustness of the functionalized material and the introduction of new functionalities made by design.[10–12] Some of these options rely on highly reactive species such as radicals,[13–15] which sometimes makes it difficult to control their high reactivity. However, other protocols are based on specific reactions between the sulphur atoms of the surface with the corresponding organic unit. The use of maleimides is included in this last group.[16] The reaction is based on the soft nucleophilicity of sulphur to react with a soft electrophile such as maleimide compounds

via a Michael addition. With this protocol, it is possible to obtain a highly efficient covalent attachment under very mild conditions, without transformation of the 2H-MoS₂ phase to the more reactive 1T-MoS₂ phase.[17,18] The use of these molecules for the functionalization of the 2H-MoS₂ phase has been proved useful with other transition metal dichalcogenides,[16] to decorate naturally occurring van der Waals heterostructures,[19] interconnect flakes,[20] and more recently for the formation of a graphene-MoS₂ covalent heterostructure where the electronic properties are dominated by the molecular interface.[21] Palma and co-workers have shown that the reaction is useful to obtain MoS₂-DNA bioconjugates.[22] Finally, Zhao and co-workers, have demonstrated that the maleimide–MoS₂ reaction is useful to tailor the electronic properties of field-effect transistors by direct on-device chemistry.[23] Now that the versatility and potential applications of this type of functionalization have been demonstrated, it is of paramount importance to obtain a detailed understanding of the on-surface covalent functionalization of MoS₂ with maleimides.

Here, we investigate in detail the maleimide–MoS₂ chemistry for the on-surface functionalization of bulk and monolayer MoS₂. The obtained organic layers are characterized using atomic force microscopy (AFM), scanning tunneling microscopy (STM), and Raman spectroscopy. The versatility of the reaction was tested at the solid–liquid interface and under ultrahigh vacuum (UHV) conditions, with two different maleimides, with and without the presence of base, allowing for structural control of the adlayer(s) covalently anchored to the MoS₂ surface.

Results and discussion

Fig. 1 shows the chemical structure of the precursors used in this work. We used a molecule with a simple structure (Bn-

ᵃDepartment of Chemistry, Division of Molecular Imaging and Photonics, KU Leuven, Celestijnenlaan 200F, 3001 Leuven, Belgium. E-mail: steven.defeyter@kuleuven.be
ᵇÁrea de Química Física, Departamento de Química, Instituto de Materiales y Nanotecnología (IMN), Universidad de La Laguna (ULL), 38200 La Laguna, Spain
ᶜDepartamento de Física de la Materia Condensada, Universidad Autónoma de Madrid, Cantoblanco 28049, Madrid, Spain. E-mail: al.vazquezdeparga@uam.es
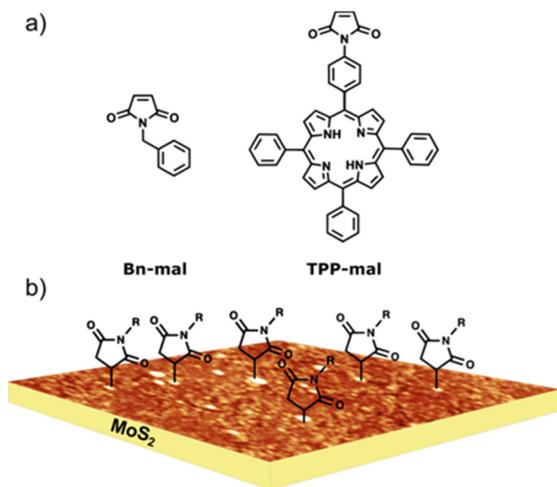*ᵈIMDEA Nanociencia, Faraday 9, 28049 Madrid, Spain.*
E-mail: emilio.perez@imdea.org
ᵉIFIMAC, Universidad Autónoma de Madrid, Cantoblanco 28049, Madrid, Spain
†Electronic supplementary information (ESI) available. See DOI: https://doi.org/10.1039/d3nr05236b

Fig. 1 (a) Molecular structures for the maleimides reagents. (b) Idealised depiction of the covalently functionalised MoS$_2$ substrate, based on experimental AFM data.

mal) and a porphyrin-derived maleimide (TPP-mal) to decorate the MoS$_2$ surface.

For the functionalization under ambient conditions, the substrates were immersed in the corresponding solution overnight (detailed information about sample preparation in the ESI†). AFM characterization of the functionalised substrates is shown in Fig. 2. Bn-succ-MoS$_2$ samples, the *N*-benzylmaleimide (Bn-mal) being converted into a succinimide upon reaction with MoS$_2$, show defined lines of organic material (Fig. 2a) with a coverage of around 30%. The distribution of the molecules indicates preferred adsorption on the edges, steps, and defects of the substrate. These lines can be found when a bare MoS$_2$ surface is imaged and can be associated to steps, terraces edges and defects on the surface (ESI S1†). The higher reactivity of the edges in 2D flakes of MoS$_2$ has been previously reported[14,24] However, we also observe a significant number of basal-plane attachments (ESI S2†). For TPP-succ-MoS$_2$, full coverage is observed (Fig. 2b) which indicates a favoured adsorption on this derivative as a result of van der Waals molecule-substrate interactions.[25] Furthermore, partial removal of the organic film with the AFM tip reveals differences in the thickness. The thickness obtained for Bn-succ-MoS$_2$ is 0.8 nm, while the one for TPP-succ-MoS$_2$ is 1.3 nm. This result is in good agreement with the larger size of the porphyrin-derived maleimide TPP-mal molecule compared to Bn-mal, this applies only when TPP-mal is attached perpendicular to the MoS$_2$ surface *via* the maleimide. With these data, we hypothesize that the direct connection of the maleimide to the porphyrinic core enhances its interaction with the MoS$_2$ basal plane when compared to Bn-mal. Maximizing the number of favourable porphyrin-porphyrin interactions can also enhance the formation of such a monolayer with increased surface coverage.

However, physisorption cannot be ruled out because AFM images show the overall surface morphology but cannot dis-
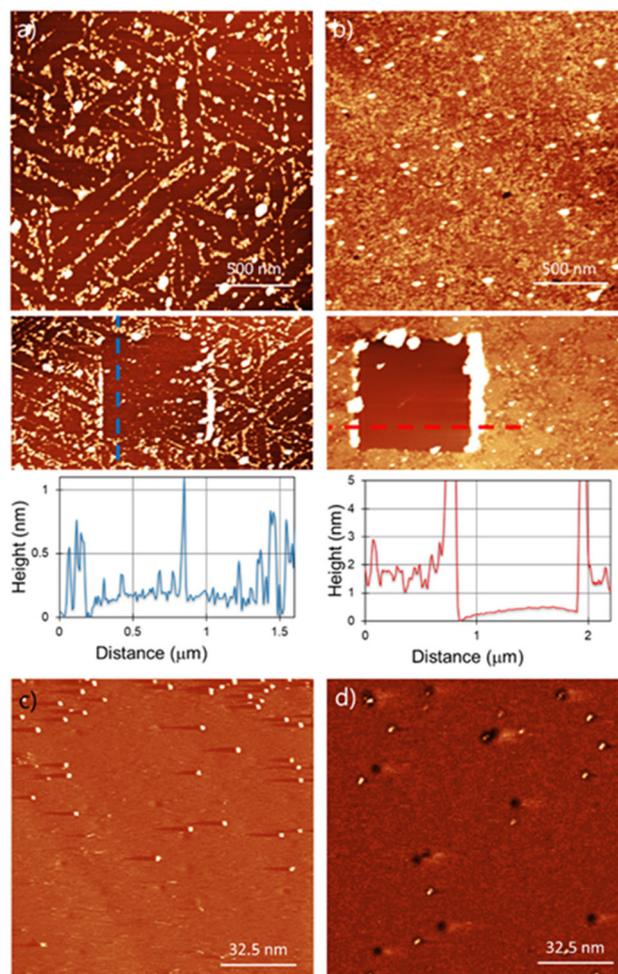
Fig. 2 AFM images (2 μm × 2 μm) for (a) Bn-succ-MoS$_2$ and (b) TPP-succ-MoS$_2$ layers on bulk MoS$_2$. A scratch on the surface was performed for the estimation of the thickness (see corresponding cross section). STM images (130 nm × 130 nm) for (c) Bn-succ-MoS$_2$ and (d) TPP-succ-MoS$_2$.

tinguish between physisorbed and covalently attached molecules. To evaluate if the organic films are covalently bonded to the MoS$_2$ surface, we used STM. STM has been widely used for the characterization of functionalization of MoS$_2$ *via* physisorption[26] or chemisorption[27,28] of molecules. Furthermore, STM is a unique technique for the detection at the molecular level of grafted units on a surface as previously demonstrated for several materials, including MoS$_2$.[29–31] Fig. 2(c) and (d) show the STM images for Bn-succ-MoS$_2$ and TPP-succ-MoS$_2$, respectively. Some black holes are observed which are a characteristic of natural MoS$_2$ and relate to point defects caused by sulphur vacancies.[32] Grafted units on the surface appear in the STM height image as bright spots. The presence of these bright spots confirms the success in the covalent modification of the MoS$_2$ surface. In any case the STM analysis is qualitative. This is due to the possibility of local removal of the grafted layer, *i.e.* nanoshaving, due to the STM tip interaction. However, the presence of covalent units even at low density,

where the Raman spectroscopy is not suitable for its detection, can be confirmed by STM, as shown in this work.

Another potentially useful feature of the reaction is that it can be tuned by addition of a base to introduce polymeric fragments, instead of single molecular attachments.[33] Fig. 3 shows the AFM results for the samples prepared by adding some drops of triethylamine (Et_3N) to the Bn-mal or TPP-mal solution.

For Bn-succ-MoS_2-Et_3N, a thicker polymeric layer of 1.8 nm can be found. The holes found on the layer go down to the MoS_2 surface as the depth is the same as the layer thickness obtained by scratching (Fig. 2a). The surface density of these holes is not homogeneous and depends on the area analyzed, as shown in large scale images (ESI S3†). For the TPP-succ-MoS_2-Et_3N, the surface is completely covered by a homogeneous layer with a thickness of around 1.8 nm. Hereby, we can confirm an increase in the thickness due to the formation of a polymeric adlayer in the presence of a base. The increased amount of material deposited on the surface was previously analyzed on liquid phase exfoliated MoS_2 using thermogravimetric analysis (TGA) and high-angle annular-dark-field scanning transmission electron microscopy (HAADF-STEM).[33] However, AFM shows not only an increase in the overall thickness of the film deposited on the surface but also the formation of larger polymeric fibers in solution that can be found in some scanned areas (ESI S4†).

To clarify the interaction of the molecules with the MoS_2 surface, we have performed the functionalization of the surface using maleimides under ultra-high vacuum (UHV) conditions. Under these conditions we have information of the crystallographic perfection and cleanliness of the MoS_2 surface at the atomic level with the added advantage of an exquisite control in the number of molecules deposited (ESI S5†). Exposing a clean MoS_2 surface to a pressure of 2.1×10^{-7} Torr for 36 minutes, corresponds to the deposition of approximately 60 Bn-maleimides for every exposed sulfur atom on the surface of the MoS_2 islands. Fig. 4 shows two STM images measured after the exposition. After the exposition to the Bn-maleimides, the surface appears cover with objects that present the same contrast at both positive and negative voltages. In contrast, defects present in the MoS_2 films as they grown display a contrast inversion in the tunneling images when going from positive to negative. The molecules have decorated the edges of the islands, the linear defects (mirror twin boundaries, MTB) and a few of them appear adsorbed in the middle of the islands.

Quantitative information about the strength in the interaction between adsorbed molecules and the surface cannot be obtained from STM imaging alone, but single molecule manipulation in UHV at cryogenic temperatures allow us to distinguish between physisorbed and chemisorbed molecules. Fig. 5(a) shows a single molecule adsorbed in the middle of a MoS_2 single layer island. There are also molecules adsorbed on the step edges and MTBs present on the island.

Fig. 5(b)–(g) shows a series of images taken during the manipulation process. For high positive bias voltages, the images show the molecule as a bright spot on the terraces as shown in Fig. 4(a) and (b). During the acquisition of these images the electrons are tunneling from the STM tip to the LUMO of the molecule and the images represent the spatial distribution of the unoccupied frontier molecular orbital. For bias smaller than +1.0 V the molecule does not appear well defined anymore because the bias voltage is lower than the energy of the LUMO and most of the electrons are tunneling directly to the substrate and the tip pushes the molecule when acquiring the images. This process creates at the position of the molecule a small bump with straight horizontal edges, as
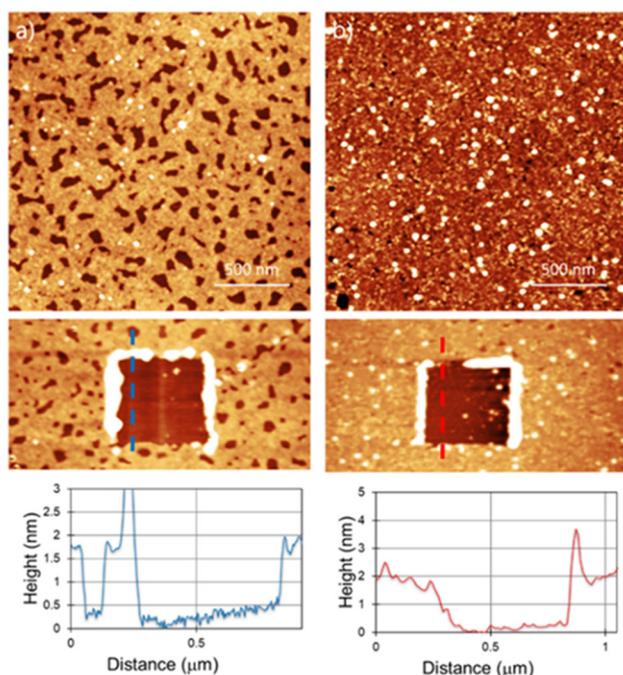

Fig. 3 AFM images (2 μm × 2 μm) for (a) Bn-succ-MoS_2-Et_3N and (b) TPP-succ-MoS_2-Et_3N layers on bulk MoS_2 in the presence of Et_3N. A scratch on the surface was performed for the estimation of the thickness (see corresponding cross section).
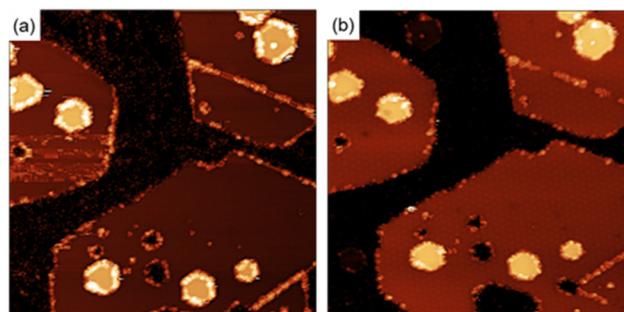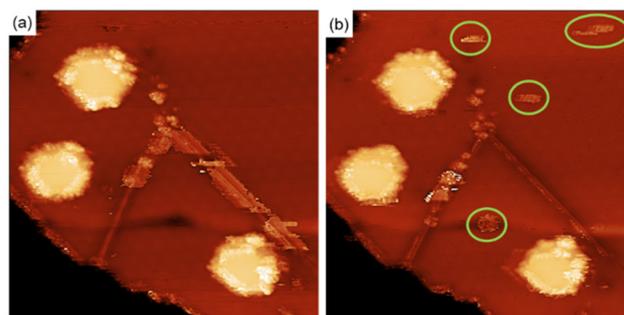

Fig. 4 STM images (100 nm × 100 nm) measured in the same area of the sample with negative bias voltage (V_b = −1.0 V, I_t = 3 pA) (a) and positive bias voltage (V_b = +1.8 V, I_t = 3 pA) (b) after exposing the MoS_2 film to a partial pressure of maleimides of 2.1×10^{-7} Torr during 36 minutes.
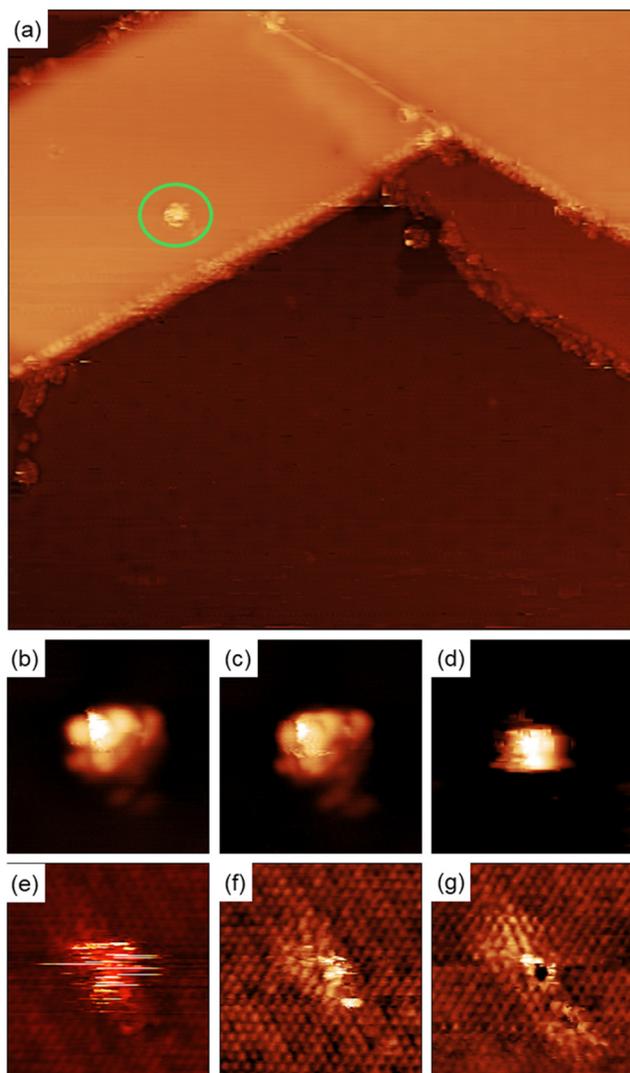
Fig. 5 (a) STM image (50 nm × 50 nm, V_b = +1.8 V, I_t = 3 pA) of a MoS_2 single layer with a maleimide adsorbed in the middle of a terrace (encircled in green) (b)–(g) STM images (7.5 nm × 7.5 nm, I_t = 50 pA) sequence of single molecule manipulation reducing the bias voltage. (b) V_b = +1.8 V, (c) V_b = +1.0 V, (d) V_b = +0.9 V, (e) V_b = +0.25 V, (f) V_b = +0.05 V, (g) V_b = +0.01 V.

Fig. 6 STM images (50 nm × 50 nm, V_b = +1.8 V, I_t = 3pA) before (a) and after (b) single molecule manipulation. The molecules removed from the domain boundary (encircled in green) appear in the terraces or at the step edges.

the resto of the sulfur atoms in the STM images, see Fig. 5(g). Adjusting the bias voltage back to +1.0 V we observe the molecule adsorbed on the same surface location shown in Fig. 5(a). This is a clear indication of the bonding between the maleimides and MoS_2 surface.

In contrast, the molecules attached to the MTBs are easily manipulated by scanning the area with high bias voltages, an indication that the interaction with the substrate is different compared with the molecules in the middle of the terraces suggesting that the molecules are physisorbed on the 1D defects (see ESI† for details). Fig. 6(b) shows the MTB after manipulation of the molecules. Once the molecules of the MTB have been removed, the structure of the MTB in the STM images looks similar than prior to exposure to maleimides. This behavior contrast with what occurred with the molecules adsorbed in the center of the terraces (see Fig. 5).

Finally, Raman spectroscopy of the bare and functionalized substrates was performed to stablish changes in the electronic structure of the material. These results are included in the ESI S6.† The characteristic active modes of 2H-MoS_2 at 383 cm^{-1} and 408 cm^{-1} were observed; after the reaction, the decrease of (2LA(M)) mode in the 450–460 cm^{-1} region, typically used as an indication of functionalization[17] does not show a significant difference, mainly due to the type of substrate used in this work (natural MoS_2) and the low density of grafted moieties. This different reactivity of surface-based systems compared to exfoliated materials is expected due to the lower number of defects or reactive sites.

Conclusions

Solid supported MoS_2 functionalization using thiol–ene chemistry has been investigated. STM and AFM at the solid–liquid interface revealed the formation of a covalently bound polymeric adlayer on the MoS_2 surface. The addition of a Lewis base to the maleimide solutions lead to an increase in the thickness, measured by scratching with the AFM tip. In order to study the interaction of single molecules with the MoS_2 surface we took advantage of the precise control achievable in

can be seen in Fig. 5(d). Further reducing the bias voltage to +0.25 V produce images where the position of the molecule is indicated by few horizontal stripes, the molecule is invisible for the tunneling electrons and the only hint of its presence is the is the noisy signal at the molecule's position, caused by the physical interaction between the STM tip and the molecule protruding from the surface. Further reducing the bias voltage to +5 mV forces the tip closer to the surface to keep the current constant and as a result, the atomic structure of the MoS_2 film begins to be resolved. While the position of the molecule is still marked with some noisy signal, see Fig. 5(f). At lower voltages (+1 mV) the atomic structure of the MoS_2 layer is better resolved and in the position of the molecule the sulfur atom below the molecule presents a different contrast to

UHV and we deposited a small number of molecules on the surface compared to the experiments carried out in solution. Molecules adsorbed on different sites of the surface (terraces, edges of the islands and linear defects) have been visualized. Quantitative information about the strength of the molecule-substrate interaction has been obtained by single molecule manipulation. Molecules adsorbed in the center of the terraces cannot be displaced from their adsorption site using the STM. Tuning the tunneling conditions to observe the electronic states of the surface sulfur atoms, shows a strong modification in its electronic structure of the sulfur atom below the adsorbed maleimide, confirming the covalent interaction previously observed by STM at the liquid–solid interface. However, molecules adsorbed on 1D surface-defects are easily removed and the MoS_2 lattice is fully recovered, an indication of physisorption. These results reveal that the molecule-substrate interaction is stronger on the basal plane and that the defects percentage on the surface will undoubtedly influence the nature of the molecule-MoS_2 interactions. The applicability of thiol–ene chemistry on solid-supported MoS_2 has been validated and provides a tool for the functionalization of surfaces focused on the development of, for instance, molecular electronic applications.

Author contributions

M.C.R.G., M.V.S., A.L.V.P., E.M.P. and S.D.F. conceived and designed the experiments. M.V.S. and A.N. prepared the maleimide compounds. M.C.R.G. and R.S. carried out the surface characterization of samples prepared under ambient conditions. I.M.I., C.R., and C.G.A. performed the analysis of samples in UHV. M.G. and F.C. supervised the UHV experiments. M.C.R.G., A.L.V.P., E.M.P. and S.D.F. supervised research and directed data analysis. M.C.R.G., A.L.V.P., E.M.P. and S.D.F. wrote the manuscript, with contributions from all authors. All authors have given approval to the final version of the manuscript.

Conflicts of interest

There are no conflicts to declare.

Acknowledgements

References

1 E. Singh, P. Singh, K. S. Kim, G. Y. Yeom and H. S. Nalwa, *ACS Appl. Mater. Interfaces*, 2019, **11**, 11061–11105.

2 H. Wang, C. Li, P. Fang, Z. Zhang and J. Z. Zhang, *Chem. Soc. Rev.*, 2018, **47**, 6101–6127.

3 E. Martínez-Periñán, T. García-Mendiola, E. Enebral-Romero, R. del Caño, M. Vera-Hidalgo, M. Vázquez Sulleiro, C. Navío, F. Pariente, E. M. Pérez and E. Lorenzo, *Biosens. Bioelectron.*, 2021, **189**, 113375.

4 S. Niu, J. Cai and G. Wang, *Nano Res.*, 2021, **14**, 1985–2002.

5 Y. Jiao, A. M. Hafez, D. Cao, A. Mukhopadhyay, Y. Ma and H. Zhu, *Small*, 2018, **14**(36), 1800640.

6 V. Yadav, S. Roy, P. Singh, Z. Khan and A. Jaiswal, *Small*, 2019, **15**(1), 1803706.

7 Z. Wang and B. Mi, *Environ. Sci. Technol.*, 2017, **51**, 8229–8244.

8 S. Karunakaran, S. Pandit, B. Basu and M. De, *J. Am. Chem. Soc.*, 2018, **140**, 12634–12644.

9 A. Stergiou and N. Tagmatarchis, *Chem. – Eur. J.*, 2018, **24**, 18246–18257.

10 R. Torres-Cavanillas, M. Morant-Giner, G. Escorcia-Ariza, J. Dugay, J. Canet-Ferrer, S. Tatay, S. Cardona-Serra, M. Giménez-Marqués, M. Galbiati, A. Forment-Aliaga and E. Coronado, *Nat. Chem.*, 2021, **13**, 1101–1109.

11 M. Morant-Giner, J. M. Carbonell-Vilar, M. Viciano-Chumillas, A. Forment-Aliaga, J. Cano and E. Coronado, *J. Mater. Chem. C*, 2021, **9**, 10975–10984.

12 S. Ippolito, A. G. Kelly, R. Furlan de Oliveira, M.-A. Stoeckel, D. Iglesias, A. Roy, C. Downing, Z. Bian, L. Lombardi, Y. A. Samad, V. Nicolosi, A. C. Ferrari, J. N. Coleman and P. Samorì, *Nat. Nanotechnol.*, 2021, **16**, 592–598.

13 E. Er, H.-L. Hou, A. Criado, J. Langer, M. Möller, N. Erk, L. M. Liz-Marzán and M. Prato, *Chem. Mater.*, 2019, **31**, 5725–5734.

14 Y. Park, S. Shin, Y. An, J.-G. Ahn, G. Shin, C. Ahn, J. Bang, J. Baik, Y. Kim, J. Jung and H. Lim, *ACS Appl. Mater. Interfaces*, 2020, **12**, 40870–40878.

15 L. Daukiya, J. Teyssandier, S. Eyley, S. El Kazzi, M. C. Rodríguez González, B. Pradhan, W. Thielemans, J. Hofkens and S. De Feyter, *Nanoscale*, 2021, **13**, 2972–2981.

16 M. Vera-Hidalgo, E. Giovanelli, C. Navío and E. M. Pérez, *J. Am. Chem. Soc.*, 2019, **141**, 3767–3771.

17 K. C. Knirsch, N. C. Berner, H. C. Nerl, C. S. Cucinotta, Z. Gholamvand, N. McEvoy, Z. Wang, I. Abramovic, P. Vecera, M. Halik, S. Sanvito, G. S. Duesberg, V. Nicolosi, F. Hauke, A. Hirsch, J. N. Coleman and C. Backes, *ACS Nano*, 2015, **9**, 6018–6030.

18 X. Chen, C. Bartlam, V. Lloret, N. Moses Badlyan, S. Wolff, R. Gillen, T. Stimpel-Lindner, J. Maultzsch, G. S. Duesberg, K. C. Knirsch and A. Hirsch, *Angew. Chem., Int. Ed.*, 2021, **60**, 13484–13492.

19 J. Villalva, S. Moreno-Da Silva, P. Villa, L. Ruiz-González, C. Navío, S. Garcia-Orrit, V. Vega-Mayoral, J. Cabanillas-González, A. Castellanos-Gomez, E. Giovanelli and E. M. Pérez, *Nanoscale Horiz.*, 2021, **6**, 551–558.

20 M. Vázquez Sulleiro, R. Quirós-Ovies, M. Vera-Hidalgo, I. J. Gómez, V. Sebastián, J. Santamaría and E. M. Pérez, *Chem. – Eur. J.*, 2021, **27**, 2993–2996.

21 M. Vázquez Sulleiro, A. Develioglu, R. Quirós-Ovies, L. Martín-Pérez, N. Martín Sabanés, M. L. Gonzalez-Juarez, I. J. Gómez, M. Vera-Hidalgo, V. Sebastián, J. Santamaría, E. Burzurí and E. M. Pérez, *Nat. Chem.*, 2022, **14**, 695–700.

22 T. Talha-Dean, K. Chen, G. Mastroianni, F. Gesuele, J. Mol and M. Palma, *Bioconjugate Chem.*, 2023, **34**, 78–84.

23 J. Miao, L. Wu, Z. Bian, Q. Zhu, T. Zhang, X. Pan, J. Hu, W. Xu, Y. Wang, Y. Xu, B. Yu, W. Ji, X. Zhang, J. Qiao, P. Samorì and Y. Zhao, *ACS Nano*, 2022, **16**, 20647–20655.

24 C. González, Y. J. Dappe and B. Biel, *J. Phys. Chem. C*, 2016, **120**, 17115–17126.

25 P. G. Moses, J. J. Mortensen, B. I. Lundqvist and J. K. Nørskov, *J. Chem. Phys.*, 2009, **130**(10), 104709.

26 L. C. Giancarlo, H. Fang, S. M. Rubin, A. A. Bront and G. W. Flynn, *J. Phys. Chem. B*, 1998, **102**, 10255–10263.

27 S. Presolski and M. Pumera, *Mater. Today*, 2016, **19**, 140–145.

28 Z. Liu, N. Hawthorne, F. Wu, N. Sheehan, N. Argibay, J. F. Curry and J. D. Batteas, *J. Phys. Chem. C*, 2022, **126**, 18266–18274.

29 A. Brown, J. Greenwood, C. J. Lockhart de la Rosa, M. C. Rodríguez González, K. Verguts, S. Brems, H. Zhang, B. E. Hirsch, S. De Gendt, A. Delabie, M. Caymax, J. Teyssandier and S. De Feyter, *Nanoscale*, 2021, **13**, 12327–12341.

30 M. C. Rodríguez González, A. Brown, S. Eyley, W. Thielemans, K. S. Mali and S. De Feyter, *Nanoscale*, 2020, **12**, 18782–18789.

31 M. C. Rodríguez González, R. Sasikumar and S. De Feyter, *Surf. Rev. Lett.*, 2021, **28**, 2140002.

32 R. Addou, L. Colombo and R. M. Wallace, *ACS Appl. Mater. Interfaces*, 2015, **7**, 11921–11929.

33 R. Quirós-Ovies, M. Vázquez Sulleiro, M. Vera-Hidalgo, J. Prieto, I. J. Gómez, V. Sebastián, J. Santamaría and E. M. Pérez, *Chem. – Eur. J.*, 2020, **26**, 6629–6634.